Supporting Information

Potential-dependent Phase Transition and Mo-enriching Surface Reconstruction of γ-CoOOH in Heterostructured Co-Mo₂C Precatalyst Enable Water Oxidation

Zongkui Kou,† *Yong Yu,*†‡ *Ximeng Liu,*† *Xiaorui Gao,*†Ŧ* *Lirong Zheng,*∥* *Haiyuan Zou,*§ *Yajun Pang,*† *Zhongyang Wang,*† *Zhenghui Pan,*† *Jiaqing He,*‡ *Stephen J. Pennycook,*† *John Wang*†*

† Department of Materials Science and Engineering, National University of Singapore, 117574 Singapore, Singapore.

‡ Department of Physics, Southern University of Science and Technology, Shenzhen 518055, China.

Ŧ Jiangsu Laboratory of Advanced Functional Materials, School of Physics and Electronic Engineering, Changshu Institute of Technology, Changshu 215500, P. R. China.

∥ Beijing Synchrotron Radiation Facility Institute of High Energy Physics, Chinese Academy of Sciences, Beijing 100049, China.

§ Department of Chemistry and Shenzhen Grubbs Institute, Southern University of Science and Technology (SUSTech), Shenzhen 518055, China.

Experimental Section

Chemicals

Cobalt nitrate hexahydrate ($Co(NO_3)_2 \cdot 6H_2O$; ≥99.0%), Zinc nitrate hexahydrate ($Zn(NO_3)_2 \cdot 6H_2O$; ≥99.0%), 2-methylimidazole (2-mIm; 99.0%), ammonium molybdate (($NH_4)_6Mo_7O_{24} \cdot 4H_2O$, 99.0%) were purchased from Sigma-Aldrich Co., Ltd. and directly used without any purification. The DI water with the resistivity of 18.25 MΩ cm^{-1} was purified with a water ultrapure cation system.

Synthesis of Co-MOFs and their derived Co nanoparticles

Cobalt-based metal organic frameworks (Co-MOFs) and the derived Co nanoparticles were prepared via a previously reported method[1]. In a typical synthesis, 0.59 g of $Co(NO_3)_2 \cdot 6H_2O$ and 1.3 g of 2-mIm were dissolved into 40 mL of DI water, respectively. The solutions were then under stirring for 2 hours. Next, the $Co(NO_3)_2$ solution was added to the 2-mIm solution and then stirred for 4 hours. Finally, the Co-MOFs were collected after repeated centrifugation (8000 rpm, 10 min) and washed 3 times with DI water, and then dried in an oven at 80 °C overnight. Co nanoparticles were prepared by annealing the Co-MOFs in the N_2 atmosphere at 800 ℃ for one hour.

Synthesis of Mo/Zn BIF and Mo₂C

Mo/Zn bimetallic imidazolate framework (Mo/Zn BIF) and holey 2D non-layered Mo_2C nanosheets were obtained by our previous method[28]. In a typical fabrication of Mo/Zn BIF, the solution of 2-mIm (1.3 g, 15.8 mmol) and $(NH_4)_6Mo_7O_{24} \cdot 4H_2O$ (1.96 g, 1.58 mmol) in DI water (40 mL) were magnetically stirred for 2.0 hours to form a homologous ligand, to which the solution of $Zn(NO_3)_2 \cdot 6H_2O$ in DI water (40 mL) was added with subsequent stirring for 4.0 hours. Afterwards, Mo/Zn MOFs were collected after repeated centrifugation (8000 rpm, 10 min) and washed 3 times with DI water, and then dried in an oven at 80 °C overnight. Mo_2C nanosheets are obtained by post-calcination of Mo/Zn BIF at 800 ˚C within a heating rate of 5 °C min^{-1} and holding for 1 hour in the N_2 atmosphere.

Synthesis of Co-Mo$_2$C heterostructure

The Co-Mo_2C heterostructure was prepared by a two-step method. In a typical preparation, the solution of 2-mIm (1.3 g, 15.8 mmol) and $(NH_4)_6Mo_7O_{24} \cdot 4H_2O$ (1.96 g, 1.58 mmol) in DI water (40 mL) were magnetically stirred for 2.0 hours to form a homologous ligand, to which the solution of $Co(NO_3)_2 \cdot 6H_2O$ in DI water (40 ml) was added with subsequent stirring for 4.0 hours. Subsequently, the resultant purple precursors were collected after repeated centrifugation (8000 rpm, 10 min) and washed 3 times with DI water, and then dried in an oven at 80 °C overnight. The Co-Mo_2C heterostructure are prepared by annealing the above precursor in a tube furnace up to 800 ˚C at a rate of 5 °C min^{-1} and holding for 1 h in the inert N_2 atmosphere.

Structural characterization

Field emission transmission electron microscopy (TEM) and high resolution TEM (HRTEM) studies were performed using a JEM 2100F transmission electron microscope operated at 200 kV. Samples were prepared by dropping ethanol dispersion of the samples onto ultrathin carbon film-coated copper TEM grids using pipettes and dried under ambient condition. Field emission scanning electron microscopy (FESEM) studies were carried out using a JEOL S4800 scan electron microscopy operated at 15 kV for obtaining FESEM images and elemental mapping. Samples for FESEM studies were deposited on Al foil taped by Cu tape on the sample holder.

High-angle aberration-corrected dark-field scan transmission electron microscopy (HAADF-STEM) with spherical aberration correction was made with a JEM 1011 transmission electron microscope operated at 200 kV. X-ray photoelectron spectroscopy (XPS) characterizations were carried out by using a VG Scientific ESCALAB 210 electron spectrometer equipped with two ultrahigh vacuum chambers. Powder X-ray diffraction (PXRD) patterns were recorded on a Rigaku diffractometer using a Cu-Kα ($\lambda = 0.15418$ nm) X-ray source operated at 45 kV and 100 mA, at a rate of 2 º/min from 5 to 80°. N_2 adsorption-desorption isotherms were measured by a Micromeritics ASAP 2020 Brunauer-Emmett-Teller (BET) analyzer. The metal content (Co and Mo in our case) was given by performing inductively coupled plasma measurement.

In-situ Raman test

A three-electrode system was used for in-situ Raman spectroscopy measurement. Co-Mo_2C catalyst supported on the carbon cloth was used as working electrode, a Pt wire as counting electrode, and a Saturated calomel electrode (SCE) as reference electrode. All electrodes were placed in a PTFE in-situ Raman electrochemical cell, with the examined sample at the top facing to the objective lens. The electrolyte used was 1M KOH, which was encapsulated in the Raman electrochemical cell. The in-situ Raman spectroscopy was performed with the LabRAM HR Evolution Raman microscopes (HORIBA). An Argon laser ($\lambda = 514$ nm, National Laser Model 800AL) was used as the excitation line. A 10X objective was used with the numerical aperture of 0.25 (Olympus U-5RE-2). The in-situ Raman spectrum were collected when the sample undergoes a potentiostatically charging from 1.1 to 1.7 V with a step of 0.15 V by using a portal electrochemical workstation. Each measurement was conducted after holding at the specific potential for 20 mins.

XANES test

The X-ray absorption fine structure spectra data were collected at 1W1B station in Beijing Synchrotron Radiation Facility (BSRF, operated at 2.5 GeV with a maximum current of 200 mA), respectively. The measurements were carried out at the Mo K-edge (20 019 eV) and LIII-

edge (2525 eV) at room temperature. All samples were pelletized as disks of 13 mm diameter with 1mm thickness using BN powder as a binder. The data acquired were processed and analyzed by Athena software.

Electrode preparation and electrochemical measurements

To prepare the catalyst ink, 10 mg of each active materials and 20 μL of Nafion solution (5 wt%) were dispersed in a mixture of 500 μL of H_2O and 480 μL of ethanol with the assistance of ultrasonication for at least 1 h. 100 μL of the ink was then drop-cast onto a clean 1 cm × 2 cm carbon paper (catalyst loading: 1 mg cm^{-2}). Electrochemical measurements were performed in a three-electrode system using an electrochemical workstation (Solartron 1470E). Hg/HgO electrode and graphite rod were used as reference and counter electrodes, respectively. The electrolyte is 1 M KOH, which was purified with reported method[2] to exclude the influence of incident Fe doping on the catalytic performance. In a typical process, 4 g of $Ni(NO_3)_2 \cdot 6H_2O$ was dissolved in 8 mL of 18.2 MΩ·cm H_2O in an acid-cleaned polypropylene centrifuge tube, followed by the addition of 40 mL of 1 M KOH into the tube to precipitate high-purity $Ni(OH)_2$. Afterward, the mixture was shaken for 30 min and the supernatant was decanted after centrifugation. The green solid was then washed with 18.2 MΩ·cm H_2O and 1 M KOH by redispersing the solid, centrifuging, and decanting the supernatant. 40 mL of 1 M KOH solution was added to the tube for purification. In brief, the solid was dispersed in KOH solution by shaking for 30 min to purify the Fe from the KOH solution, followed by 3 h of rest. The purified KOH solution was decanted after centrifugation and transferred to an acid polypropylene bottle. Linear sweep voltammetry with a scan rate of 5 mV s^{-1} was conducted at room temperature. For Tafel plot, the linear portion is fit to the Tafel equation. All the potentials reported in the present study were converted to a reversible hydrogen electrode (RHE) scale via an equation as follows: $E_{RHE} = E_{SCE} + 0.098 + 0.059 \times pH$ (pH≈13.88). The long-term stability was also tested at the varied overpotentials. EIS was performed at the open-circuit voltage with frequency from

0.01 to 100 000 Hz and an amplitude of 10 mV under the overpotential of 200 mV. EIS spectra were fitted by the ZView software.

TOF calculations

The turnover frequency (TOF) at a given overpotential was calculated using the following formula:

$$\text{TOF} = \frac{\text{number of } O_2 \text{ turnovers}}{\text{number of metal ions}} \tag{1}$$

The number of O_2 turnovers was calculated using the current density at 300 mV overpotential via:

$$\text{Number of } O_2 \text{ turnovers} = \left(j\frac{mA}{cm^2}\right)(1cm^2)\left(\frac{\frac{1C}{s}}{1000\ mA}\right)\left(\frac{1\ mol\ e^-}{96,\ 485\ C}\right) \times \left(\frac{1\ mol\ O_2}{4\ mol\ e^-}\right)\left(\frac{6.02 \times 10^{23}\ mol\ O_2}{1\ mol\ O_2}\right)$$

$$= 1.56 \times 10^{15} j\ (s^{-1}) \tag{2}$$

The total number of metal ions was determined from ICP analysis.
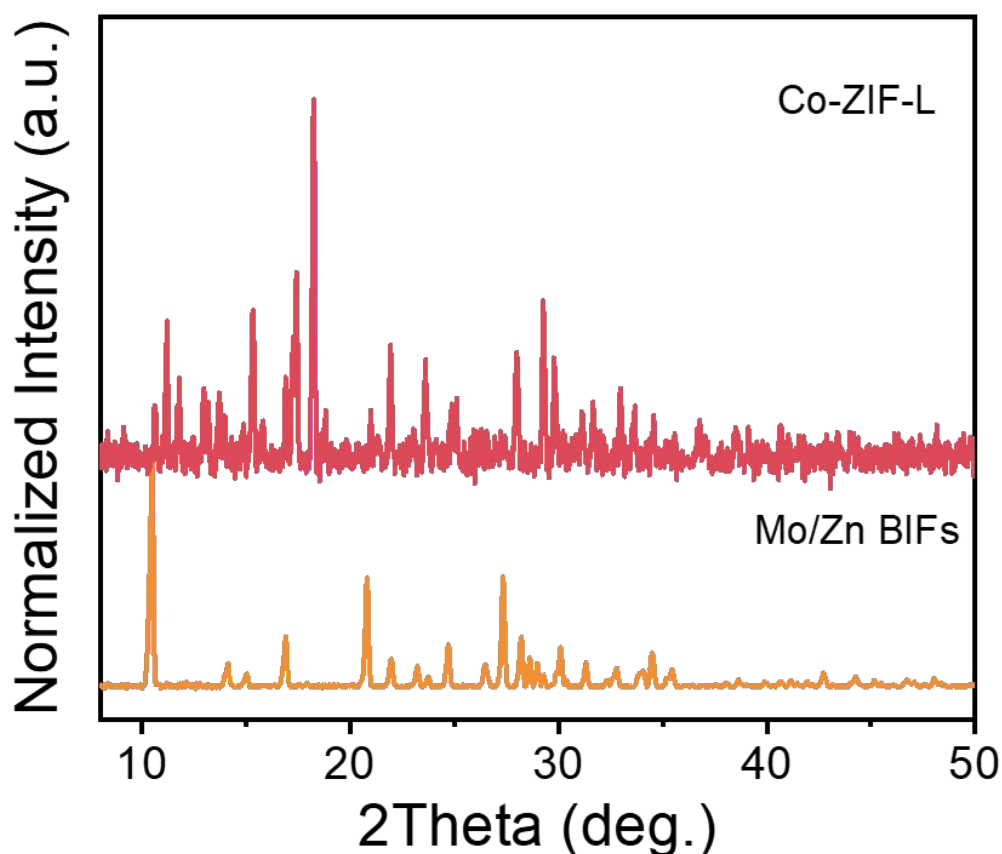
Figure S1. XRD pattern of Mo/Zn BIFs and Co-ZIF-L precursors which are used to derive the Mo$_2$C and Co nanoparticles at the same conditions.
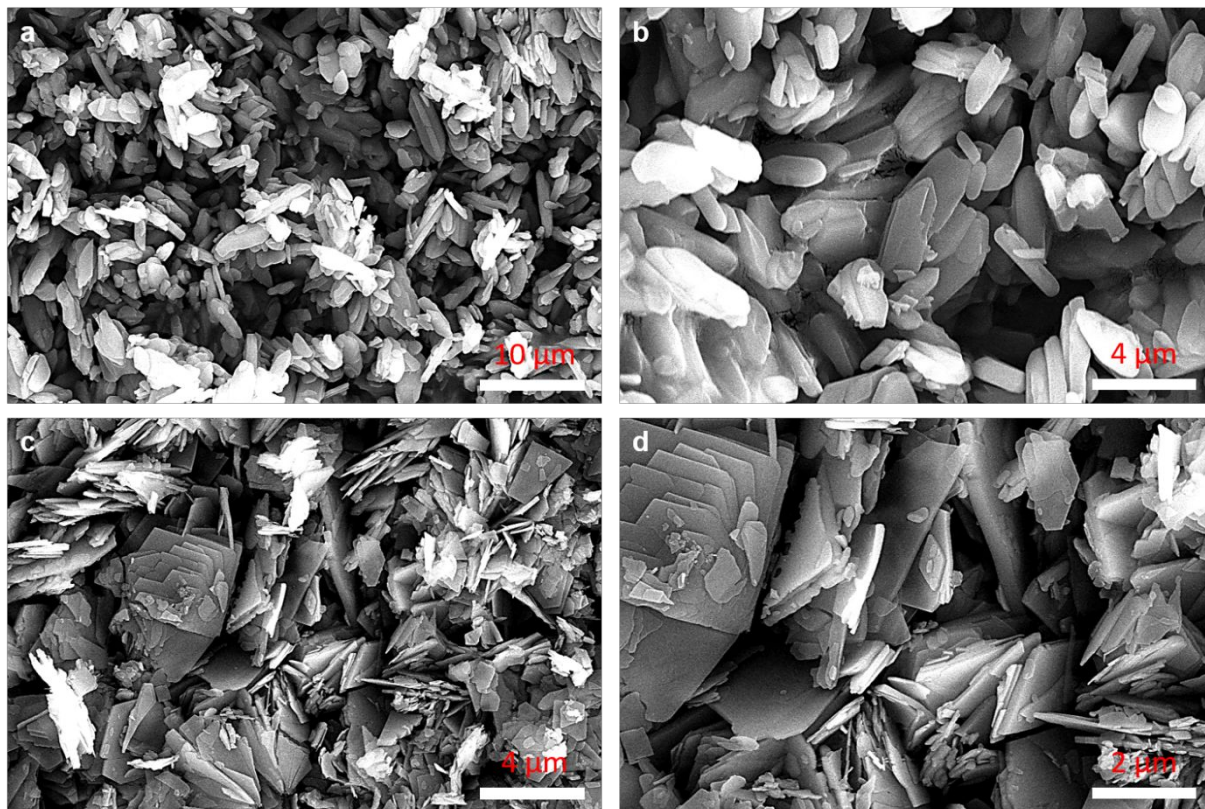
Figure S2. SEM images of Co-ZIF-L (a, b) and Mo/Zn BIFs (c, d) precursors both of which show the sheet-like morphology.
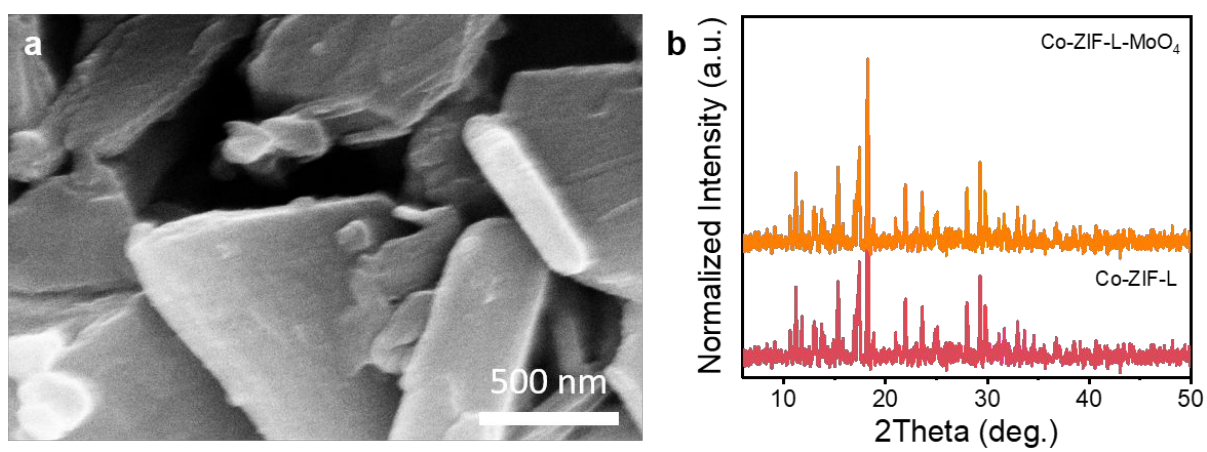
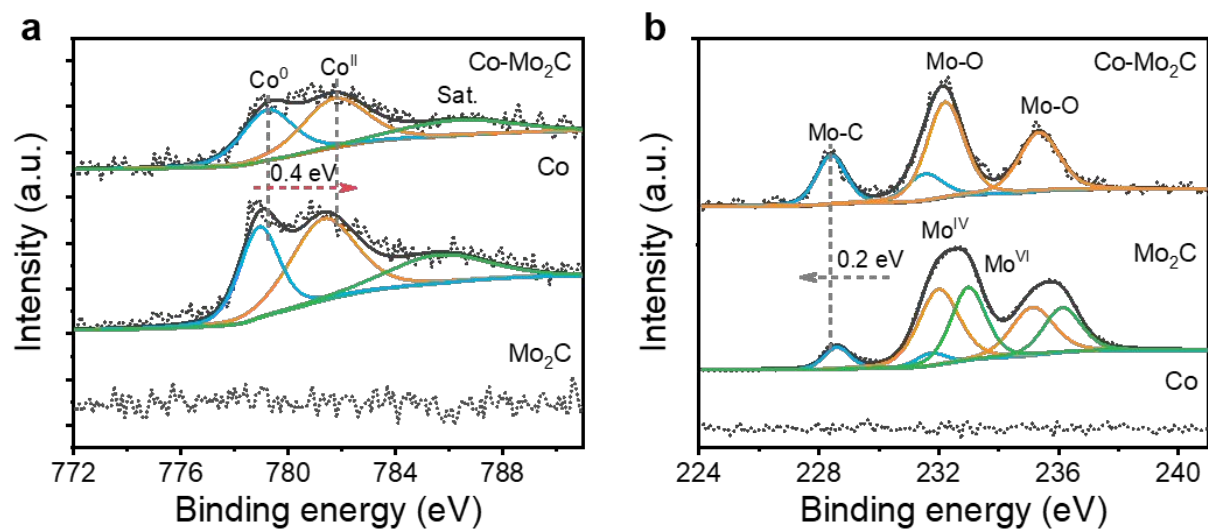**Figure S3.** SEM image (a) and XRD pattern (b) of Co-ZIF-L-MoO$_4$.

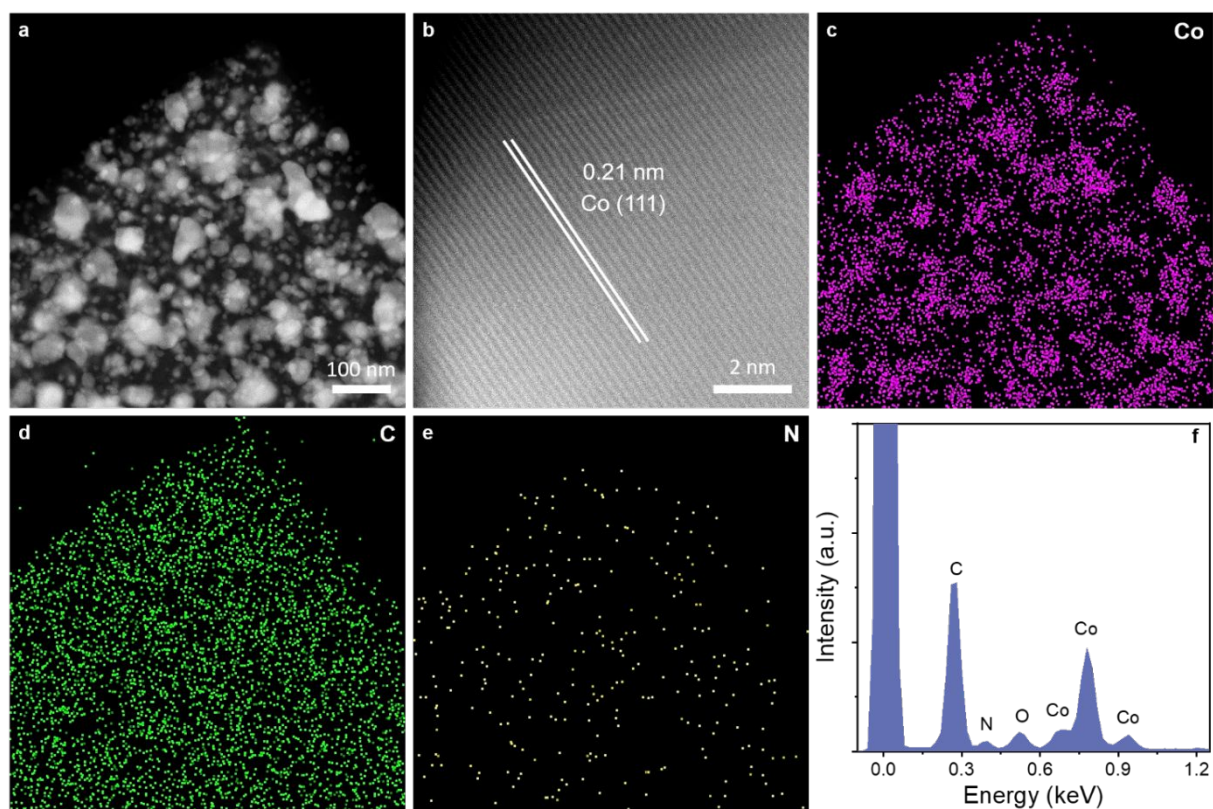**Figure S4.** Deconvoluted Co 2p (a) and Mo 3d (b) XPS spectra of Co-Mo$_2$C, Mo$_2$C and Co.

Figure S5. The STEM image (a) of Co nanoparticles and the corresponding high-resolution STEM image (b), EDS maps (c-e) as well as EDS spectra (f). Clearly, Co nanoparticles of uneven sizes are uniformly loaded on the nitrogen-doped carbon.
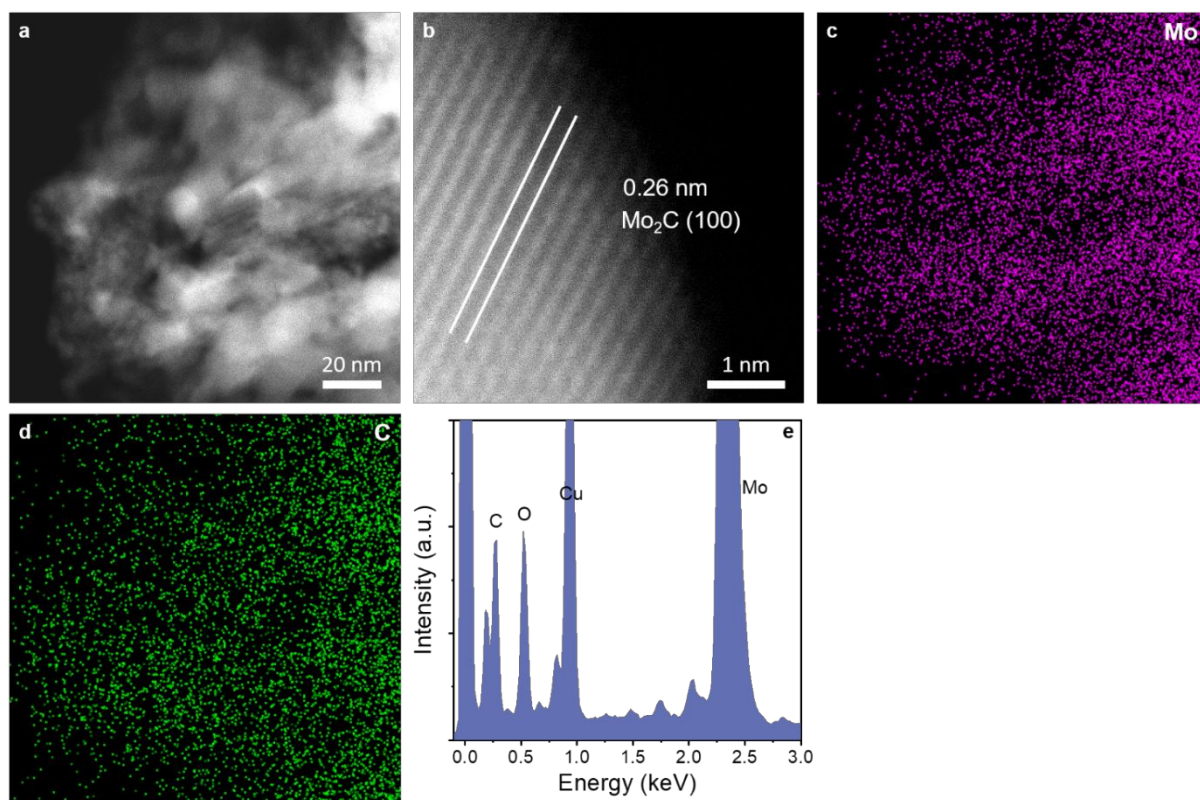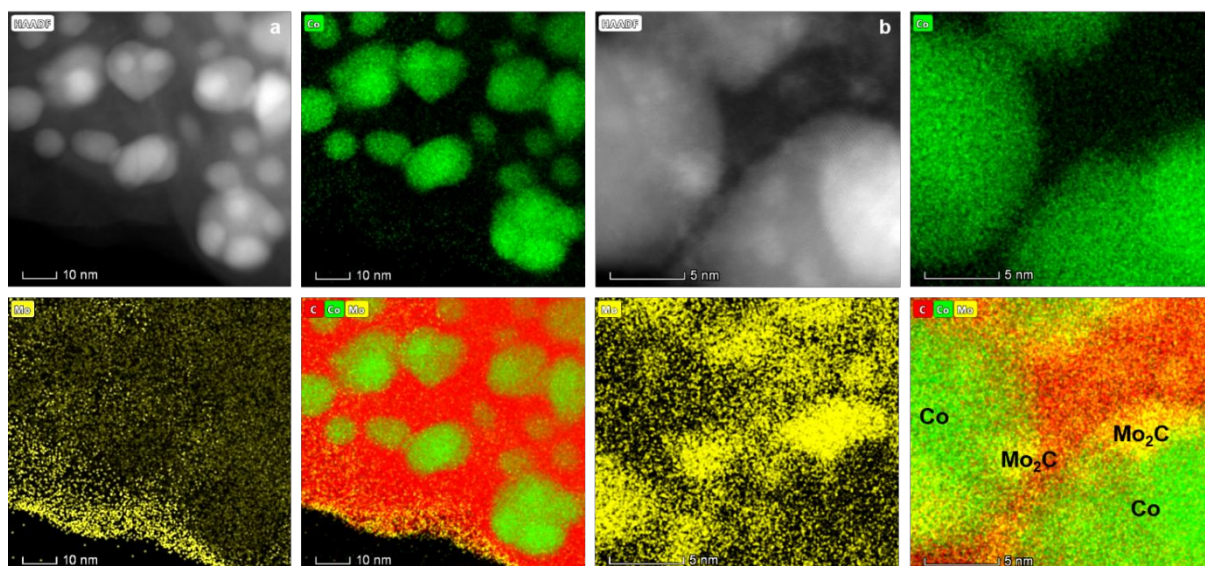
Figure S6. The STEM image (a) of Mo_2C nanoparticles and the corresponding high-resolution STEM image (b), EDS maps (c, d) as well as EDS spectra (e). Similar to Co, Mo_2C nanoparticles also have uneven sizes.

Figure S7. The HAADF-STEM image and elemental mapping of Co-Mo₂C heterostructure.
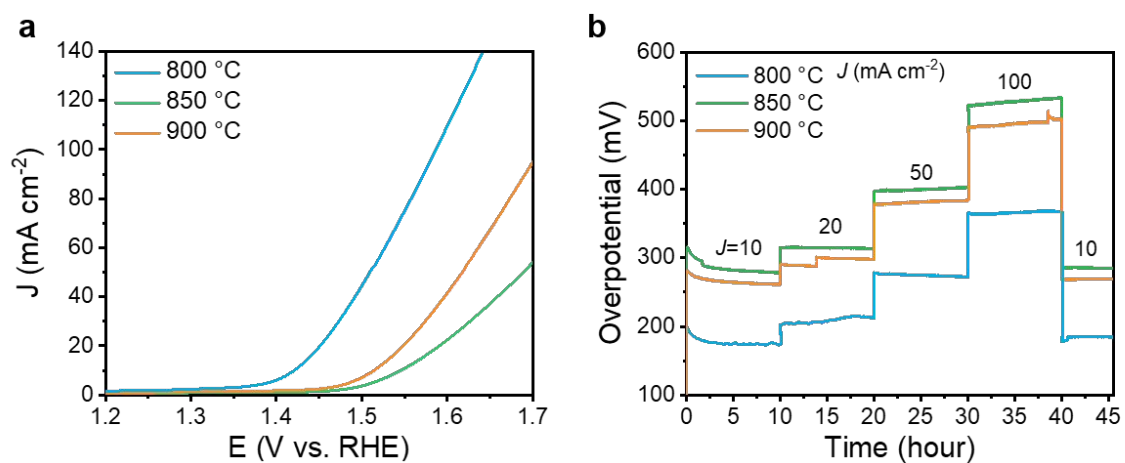
Figure S8. The LSV curves (a) of the products obtained at different temperatures and overpotential-time response curves (b) at varying current densities.
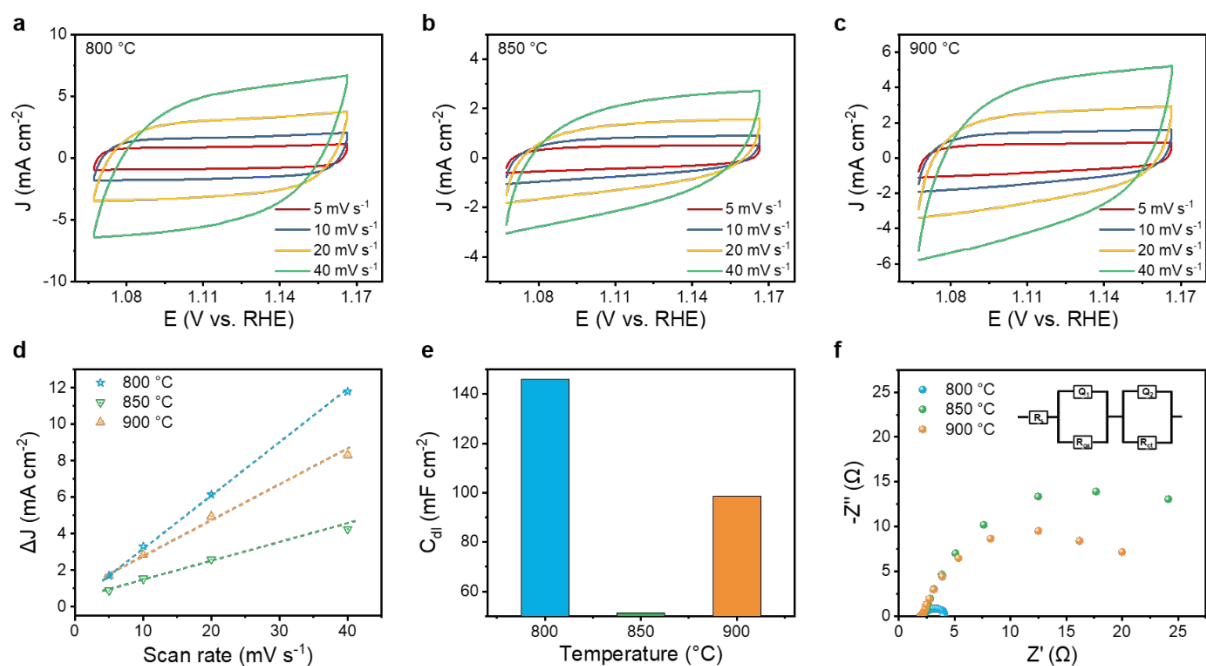
Figure S9. The CV curves at various scan rates (a-c), the corresponding current density difference (ΔJ) at 1.117 V vs RHE as a function of scan rate (d), calculated C_{dl} values (e) and electrochemical impedance spectra inserted with equivalent circuit diagram (f) of the products obtained at different temperatures.
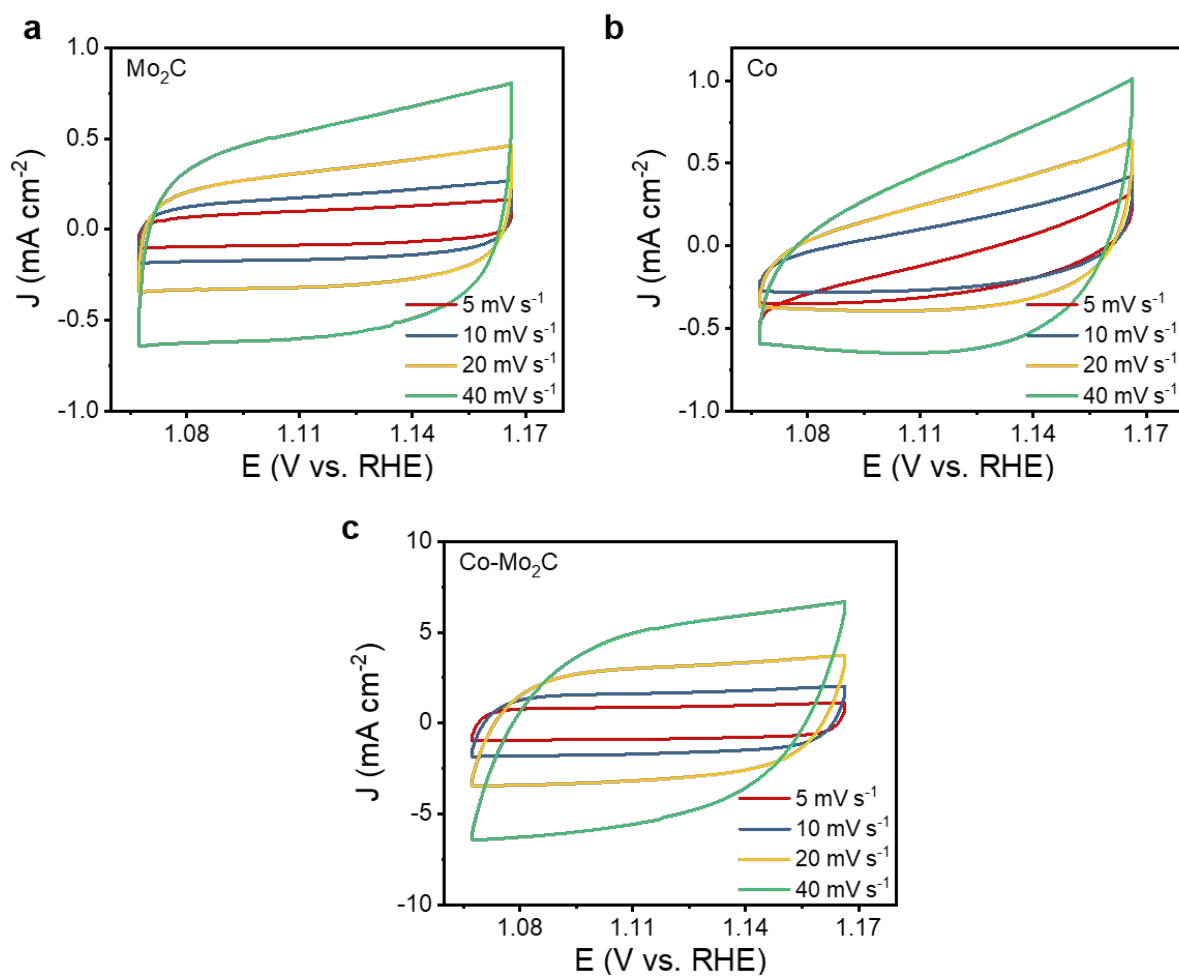
Figure S10. The CV curves at various scan rates of Mo_2C (a), Co (b) and Co-Mo_2C heterostructure (c).
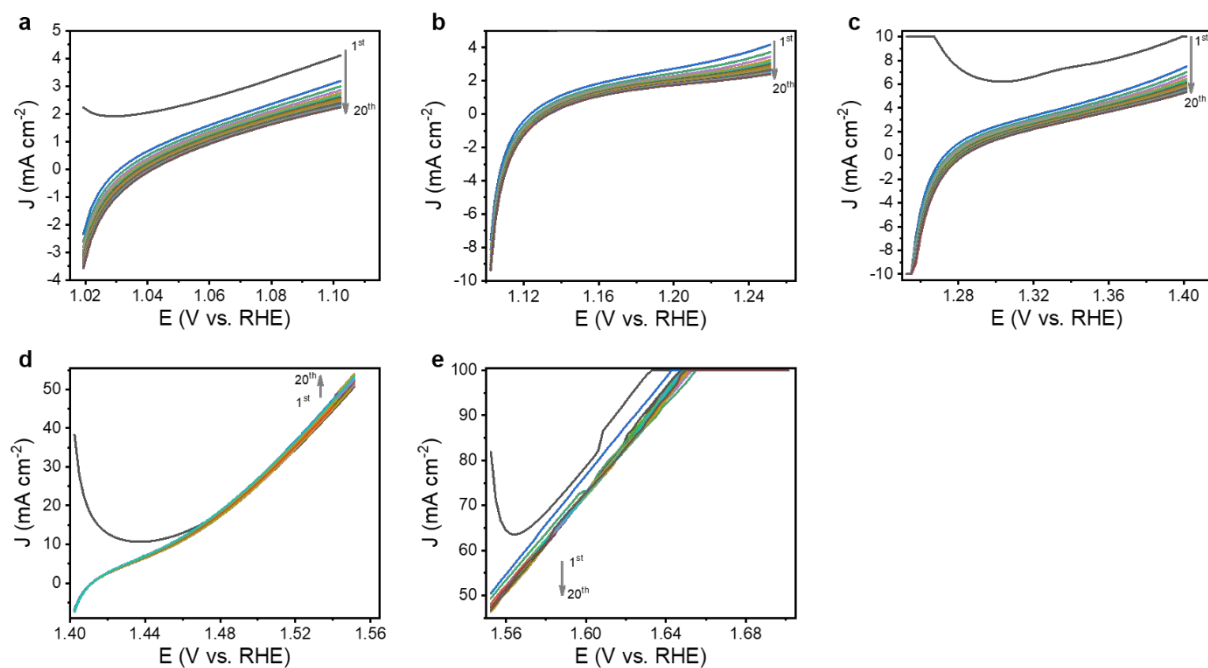
Figure S11. The LSV curves at different potential intervals of 1.02-1.10 V (a), 1.10-1.25 V (b), 1.25-1.40 V (c), 1.40-1.55 V (d) and 1.55-1.70 V (e). Note that we have set a current density terminate of 100 mA cm^{-2} to weaken the influence of mass oxygen bubbles on operando Raman tests.
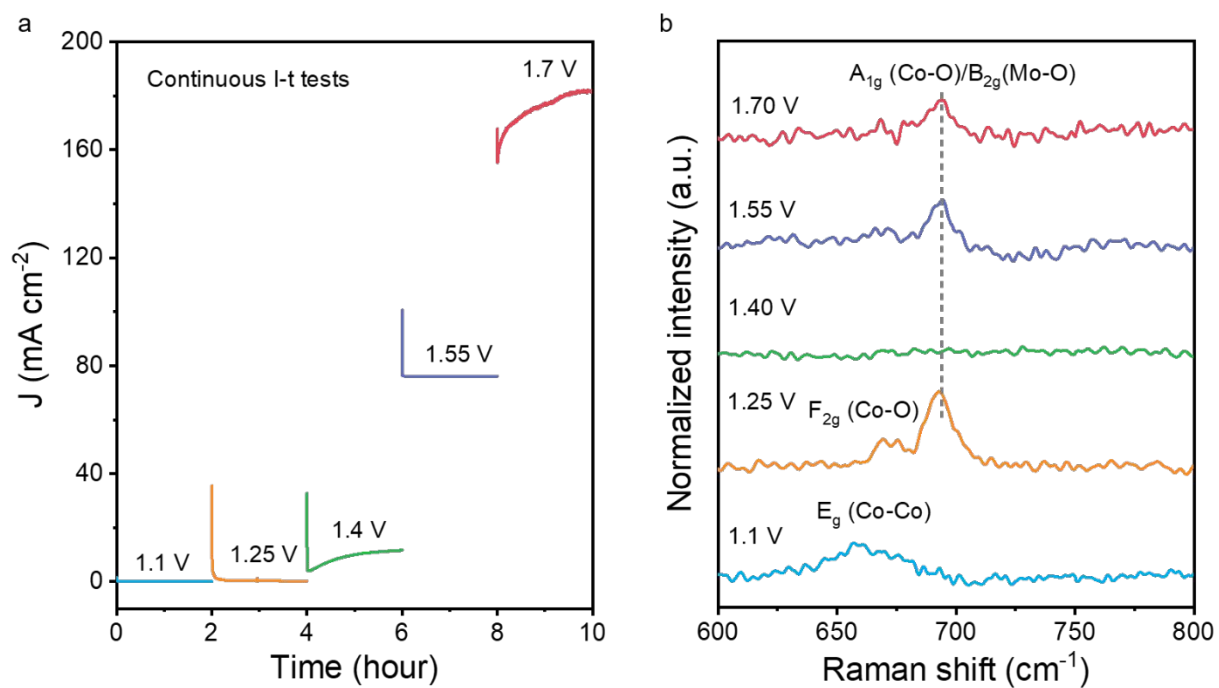
Figure S12. Current-time response curves (a) of Co-Mo$_2$C heterostructure at different applied potentials for each 2.0 hours. (b) The corresponding *ex situ* Raman spectra from 600-800 cm^{-1}.
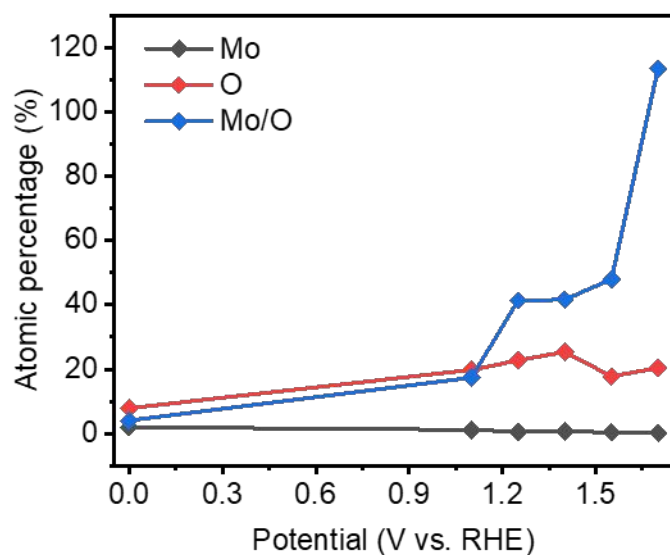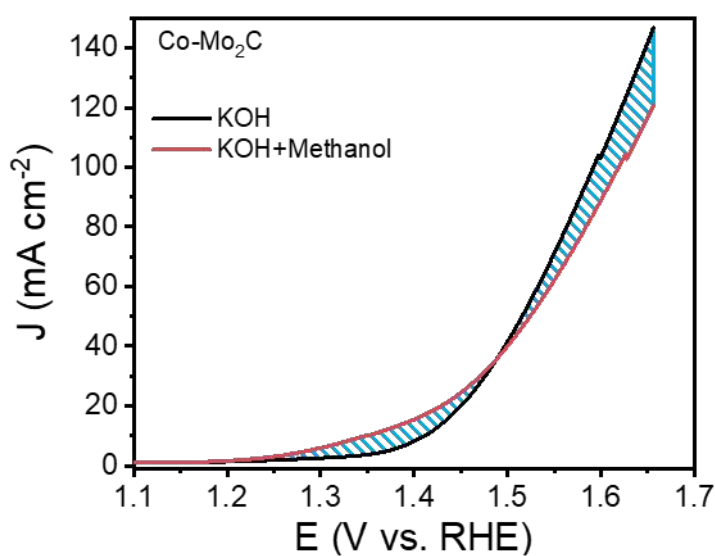
Figure S13. Atomic percentage calculated by XPS data.

Figure S14. Comparison of LSV curves of Co-Mo$_2$C heterostructure in 1 M KOH with and without methanol (1 mL). Scan rate: 5 mV s^{-1}. Direction of scanning is from low to high potential.

References

[1] Zang,W.; Sumboja, A.; Ma, Y.; Zhang, H.; Wu, Y.; Wu, S.; Wu, H.; Liu, Z.; Guan, C.; Wang, J. Single Co Atoms Anchored in Porous N-Doped Carbon for Efficient Zinc-Air Battery Cathodes. *ACS Catal.* **2018**, *8*, 8961-8969.

[2] Trotochaud, L.; Young, S. L.; Ranney, J. K.; Boettcher, S. Nickel-Iron Oxyhydroxide Oxygen-Evolution Electrocatalysts: The Role of Intentional and Incidental Iron Incorporation. *J. Am. Chem. Soc.* **2014**, *136*, 6744-6753.